Available online at www.sciencedirect.com
SCIENCE DIRECT
ELSEVIER
Journal of the European Ceramic Society 26 (2006) 2075–2079
ECERS
www.elsevier.com/locate/jeurceramsoc

Crystal structure–microwave dielectric property relations in $Sm(Nb_{1-x}Ta_x)(Ti_{1-y}Zr_y)O_6$ ceramics

Takeshi Oishi [a,*], Akinori Kan [a], Hitoshi Ohsato [b], Hirotaka Ogawa [a]

[a] *Faculty of Science and Technology, Meijo University, 1-501 Shiogamaguchi, Tempaku-ku, Nagoya 468-8502, Japan*
[b] *Materials Science and Engineering, Shikumi College, Nagoya Institute of Technology, Gokiso-cho, Showa-ku, Nagoya 466-8555, Japan*

Available online 14 November 2005

Abstract

The effects of the Ta substitution for Nb and the Zr substitution for Ti on the microwave dielectric properties and crystal structure of $Sm(Nb_{1-x}Ta_x)(Ti_{1-y}Zr_y)O_6$ ceramics were investigated in this study. The $Sm(Nb_{1-x}Ta_x)TiO_6$ ($x=0$–1) ceramics were single phase, whereas the limit of solid solutions for the $SmTa(Ti_{1-y}Zr_y)O_6$ ceramics was $y=0.4$. In the case of the $Sm(Nb_{1-x}Ta_x)TiO_6$ ceramics, the dielectric constant and the temperature coefficient of resonant frequency were decreased, whereas the quality factor was increased by the Ta substitution for Nb. The maximum $Q\cdot f$ value was obtained when the $SmTaTiO_6$ was synthesized, and the microwave dielectric properties are, $\varepsilon_r=37.6$; $\tau_f=24.2$ ppm/°C; and $Q\cdot f=24541$ GHz. On the other hand, the dielectric constants of the $SmTa(Ti_{1-y}Zr_y)O_6$ ceramics were decreased from 37.6 to 28.9, whereas the quality factor was increased from 24541 to 38320 GHz with increasing composition y from 0 to 0.4. The temperature coefficient of resonant frequency of the ceramics varied from 24.2 to −11.6 ppm/°C. A near zero temperature coefficient of resonant frequency results from the composition of $y=0.3$ with a dielectric constant of 31.1 and $Q\cdot f$ value of 37481 GHz.
© 2005 Elsevier Ltd. All rights reserved.

Keywords: Powders-solid state reaction; X-ray method; Dielectric properties; ZrO_2

1. Introduction

A number of dielectric ceramics have been developed for application in the area of mobile and satellite communication systems. Typical dielectric resonator ceramics are required to have a high dielectric constant ($\varepsilon_r>25$), a low dielectric loss or high Q ($Q=1/\tan\delta>5000$ between 5 and 10 GHz), and a near zero temperature coefficient of resonant frequency ($\tau_f=0\pm5$ ppm/°C).[1] Recently, $SmNbTiO_6$ ceramic[2] has been reported to be a useful material for the dielectric resonator application; the dielectric constant of the ceramics is comparable to that of $Ba_2Ti_9O_{20}$ ceramic[3] that is widely used for the dielectric resonator in the base station. However, since the $Q\cdot f$ value of $SmNbTiO_6$ ceramic is lower than that of $Ba_2Ti_9O_{20}$ ceramic, an improvement in the $Q\cdot f$ value of $SmNbTiO_6$ ceramic is required for a commercial application. Moreover, as the τ_f value of $SmNbTiO_6$ ceramic has been reported to possess a large positive value; the improvement in τ_f value is also required for the application as the dielectric resonator. Thus, in order to improve these dielectric properties and clarify the relationship between crystal structure and microwave dielectric properties, the influence of Ta substitution for Nb and Zr substitution for Ti on the microwave dielectric properties and the crystal structure of $SmNbTiO_6$ ceramic has been investigated in this study. Although it is known that the crystal structure of $SmNbTiO_6$ ceramic had the aeschynite-type structure (S.G. *Pnma*),[4] the details on the relationship between the crystal structure and microwave dielectric properties have not been evaluated to date.

2. Experimental

High purity (>99.9%) Sm_2O_3, Nb_2O_5, Ta_2O_5, TiO_2 and ZrO_2 powders were processed using the solid-state reaction method to form $Sm(Nb_{1-x}Ta_x)(Ti_{1-y}Zr_y)O_6$ ceramics. These powders weighed on the basis of the stoichiometric composition were mixed with acetone and calcined at 1250 °C for 4 h in air. These calcined powders were crushed and ground with polyvinyl alcohol, and then formed into pellets with 12 mm in diameter and 7 mm thick under a pressure of 100 MPa. These pellets were sintered at the various temperatures ranging from 1375 °C to 1650 °C for 10 h in air with heating and cooling rates of 5 °C/min. Subsequently, these pellets were polished and annealed at 850 °C for 2 h in air. The phases of the sintered

* Corresponding author.

0955-2219/$ – see front matter © 2005 Elsevier Ltd. All rights reserved.
doi:10.1016/j.jeurceramsoc.2005.09.062

specimens were identified by X-ray powder diffraction (XRPD), using Cu Kα filtered through Ni foil. The lattice parameters and crystal structures of the ceramics were refined in terms of the Rietveld analysis.[5,6] The bond lengths and volumes of the polyhedra were determined from the refined crystal structure parameters. The microwave dielectric properties (ε_r and tan δ) in the frequency range of 6.2–9.0 GHz were examined by Hakki and Coleman method.[7] The temperature coefficient of resonant frequency (τ_f) of the sample was determined from the resonant frequency at the two temperatures of 20 °C and 80 °C. Moreover, the microstructure of the samples was investigated in terms of field emission scanning electron microscopy (FE-SEM) and energy dispersive X-ray (EDX) analysis.

3. Results and discussion

From the XRPD patterns, the $Sm(Nb_{1-x}Ta_x)TiO_6$ ceramics were single phase over the whole composition range. In order to clarify the effect of Ta substitution for Nb on the crystal structure of $Sm(Nb_{1-x}Ta_x)TiO_6$ ceramics, the lattice parameters of the samples were refined by Rietveld analysis and the results are shown in Fig. 1 as a function of composition x. A linear dependence of the lattice parameter on composition x was observed; the lattice parameter, a, linearly decreased with the Ta substitution for Nb, whereas the lattice parameters, b and c, increased. Any remarkable variations in the lattice parameters caused by the Ta substitution for Nb were not observed, because the ionic radii of Nb^{5+} and Ta^{5+} reported by Shannon[8] are similar values when the coordination number is six. From the results of variations in the lattice parameters, it is considered that the $Sm(Nb_{1-x}Ta_x)TiO_6$ ceramics form the solid solutions because the linear variations in the lattice parameters satisfy the Vegard's law which confirms the formation of solid solutions.

The effects of the Ta substitution for Nb on the microwave dielectric properties of $Sm(Nb_{1-x}Ta_x)TiO_6$ ceramics are listed in Table 1 as a function of x. The dielectric constants of the samples decreased from 43.3 to 37.6, whereas the $Q \cdot f$ values slightly increased from 15866 to 24541 GHz with the Ta substitution for Nb. Moreover, the temperature coefficients of resonant frequency of the samples ranged from 39.8 to 24.2 ppm/°C. Thus, it is considered that additional modifications are required for dielectric resonator applications since the τ_f values of the samples are not sufficiently close to 0 ppm/°C. In order to improve these dielectric properties of the samples, the Zr substitution for Ti was performed for the $SmTaTiO_6$ ceramic because the $Q \cdot f$ values were increased by Ta substitution for Nb, and the maximum value is obtained at $x = 1$, i.e., $SmTaTiO_6$ ceramic.

Table 1
Microwave dielectric properties of $Sm(Nb_{1-x}Ta_x)TiO_6$ ceramics

Composition x	ε_r	$Q \cdot f$ (GHz)	τ_f (ppm/°C)
0	43.3	15866	39.8
0.25	41.6	18916	35.7
0.5	39.3	19633	32.5
0.75	38.5	22119	26.4
1	37.6	24541	24.2

The XRPD patterns of $SmTa(Ti_{1-y}Zr_y)O_6$ ceramics obtained in the temperature range of 1475 °C–1650 °C are shown in Fig. 2. All the samples with the compositions ranging from 0 to 0.4 showed a single phase, whereas those synthesized at a higher composition than $y = 0.4$ contained the $SmTaO_4$ and ZrO_2 phases. Therefore, these results suggest that the limit of solid solutions may be approximately $y = 0.4$. Moreover, in the single phase region, i.e., $0 \le y \le 0.4$, there are small shifts of the diffraction peaks to lower angular side of 2θ by the Zr substitution for Ti; this implies that the lattice parameters of the samples

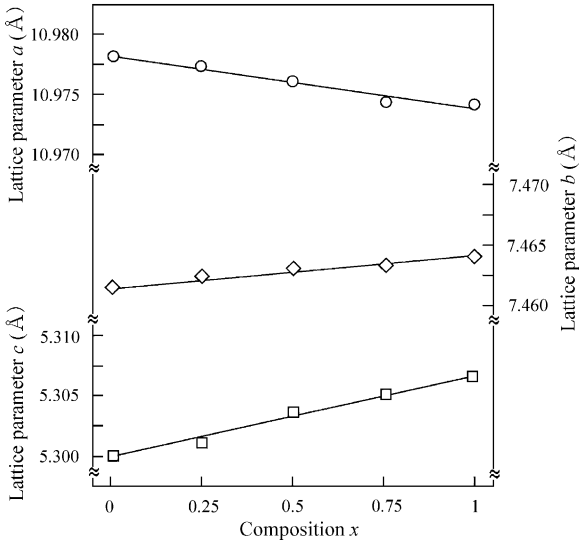

Fig. 1. Effect of Ta substitution for Nb on lattice parameters of $Sm(Nb_{1-x}Ta_x)TiO_6$ ceramics as a function of composition x.

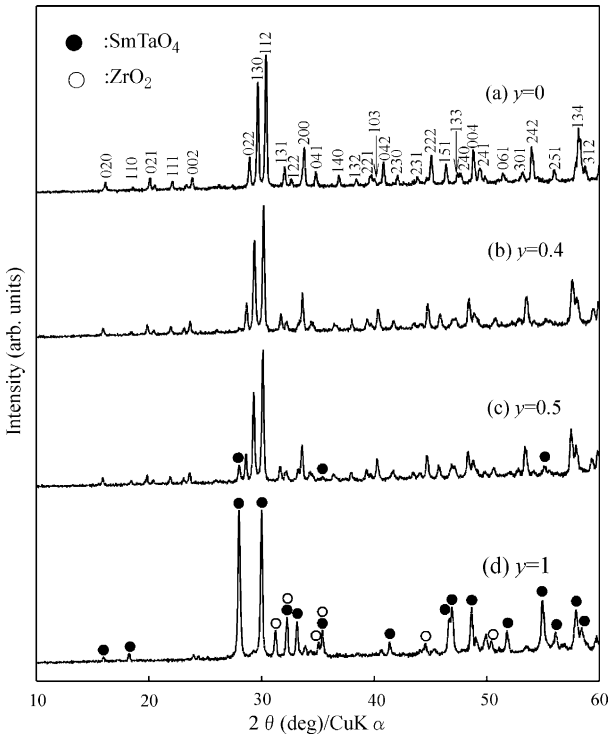

Fig. 2. XRPD patterns of $SmTa(Ti_{1-y}Zr_y)O_6$ ceramics at: (a) $y = 0$; (b) $y = 0.4$; (c) $y = 0.5$; and (d) $y = 1$.

Table 2
Lattice parameters and unit cell volumes of $SmTa(Ti_{1-y}Zr_y)O_6$ ceramics

Composition y	Lattice parameters (Å)			Unit cell volumes (Å^3)
	a	b	c	
0	10.97464	7.46409	5.30670	434.702
0.1	11.01246	7.47925	5.31234	437.551
0.2	11.04669	7.49430	5.31908	440.352
0.3	11.08954	7.51230	5.32692	443.774
0.4	11.12091	7.52654	5.33232	446.326

increased with increasing composition y. Thus, in order to clarify the effect of Zr substitution for Ti on the crystal structure of the samples, the lattice parameters and unit cell volumes of the samples were refined by the Rietveld analysis and the results are listed in Table 2. All the lattice parameters of $SmTa(Ti_{1-y}Zr_y)O_6$ ceramics linearly increased with increasing composition y up to $y = 0.4$, and the variation in the lattice parameter, a, is remarkable in comparison with that of lattice parameters, b and c. As a result, the unit cell volumes of the samples increased; these results were related to the differences in the ionic radii between Ti^{4+} and Zr^{4+} ions because the ionic radius of Zr^{4+} ion is larger than that of Ti^{4+} ion when the coordination number is six. The crystal structure of $SmTa(Ti_{1-y}Zr_y)O_6$ ceramics is composed of SmO_8 polyhedron and $(Ta,Ti,Zr)O_6$ octahedron; these crystal structures are shown in Fig. 3. The effects of Zr substitution for Ti on the volumes of the polyhedra in the $SmTa(Ti_{1-y}Zr_y)O_6$ ceramics are shown in Fig. 4. The volumes of SmO_8 and $(Ta,Ti,Zr)O_6$ polyhedra were determined on the basis of the refined atomic distances in these polyhedra. The variations in the volume of the SmO_8 polyhedra and the $(Ta,Ti,Zr)O_6$ octahedra were slightly increased in

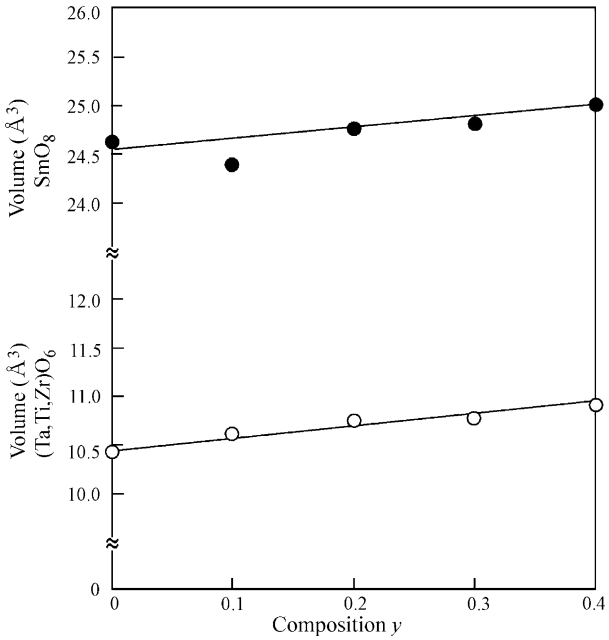

Fig. 4. Variations in volume of SmO_8 polyhedron and $(Ta,Ti,Zr)O_6$ octahedron.

$SmTa(Ti_{1-y}Zr_y)O_6$ ceramics by the Zr substitution for Ti. Thus, the increase in the unit cell volume of the $SmTa(Ti_{1-y}Zr_y)O_6$ in the single phase region is considered to relate with the variations in the volume of both SmO_8 polyhedra and $(Ta,Ti,Zr)O_6$ octahedra.

The effects of Zr substitution for Ti on the variations in the covalency of cation-oxygen bonds of the $SmTa(Ti_{1-y}Zr_y)O_6$ ceramics in the single phase region were calculated from the bond valence theorem.[9] Thus, the variation in the covalency of

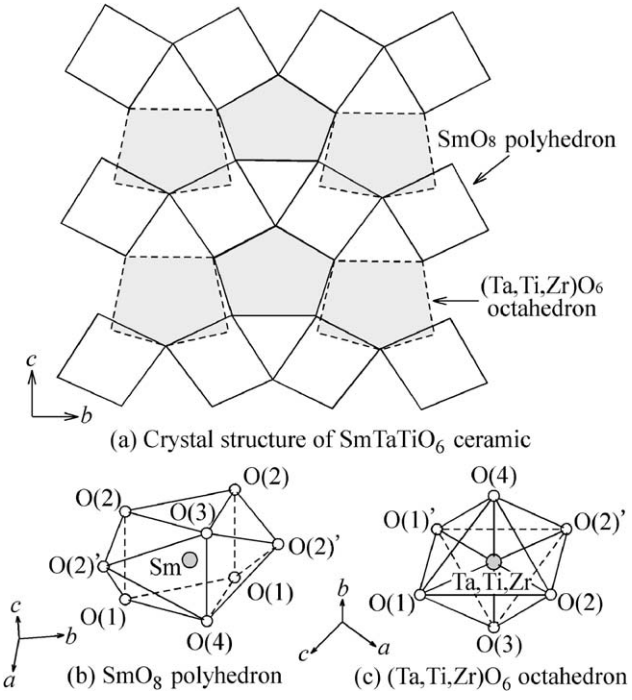

Fig. 3. Schematic diagram on crystal structures of: (a) $SmTaTiO_6$ ceramic; (b) SmO_8 polyhedron; and (c) $(Ta,Ti,Zr)O_6$ octahedron.

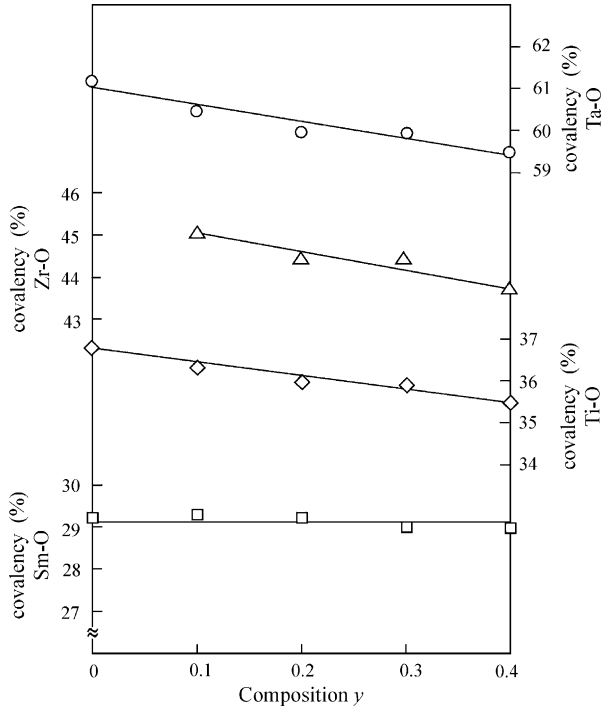

Fig. 5. Effect of Zr substitution for Ti on covalencies of cation-oxygen bond as a function of composition y.

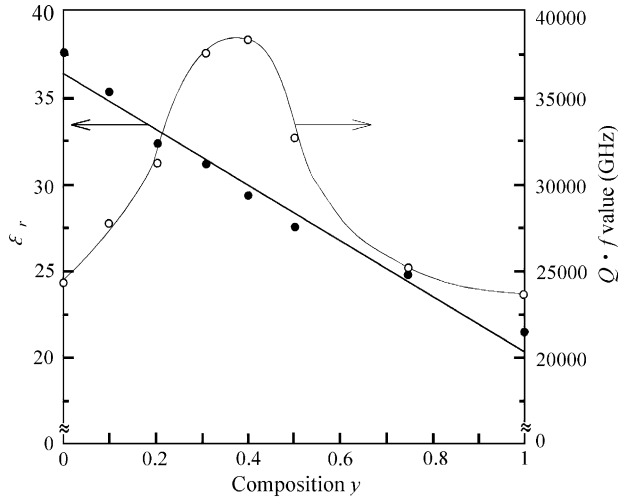

Fig. 6. Variations in dielectric constant and $Q \cdot f$ values of $SmTa(Ti_{1-y}Zr_y)O_6$ ceramics as a function of composition y.

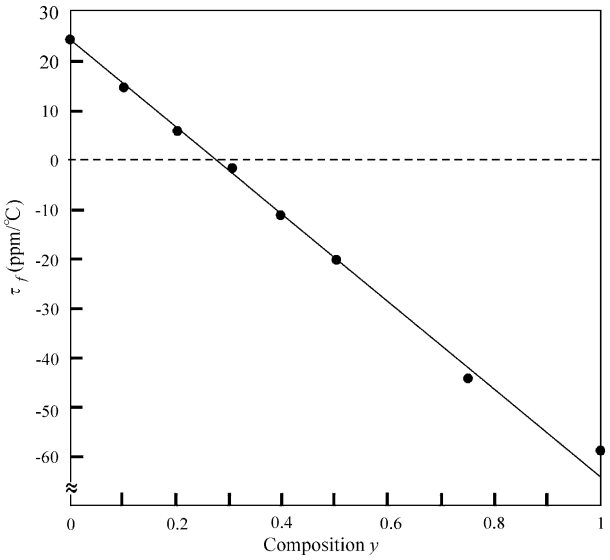

Fig. 7. Temperature coefficient of resonant frequency of $SmTa(Ti_{1-y}Zr_y)O_6$ ceramics.

the cation-oxygen bond was calculated by using the refined bond length and the relationship between covalency and bond length is given by two equations:

$$s = \left(\frac{R}{R_1}\right)^{-N} \tag{1}$$

$$f_c = \mathrm{as}^M \tag{2}$$

where s is the bond strength, R the refined bond length, R_1 the empirical constant which depends on the cation site and N is the constant which is different for each cation-anion pair. Moreover, a and M in Eq. (2) are the empirically determined parameters in order to estimate the covalency of cation-oxygen bond. The covalencies of the cation-oxygen bonds in the SmO_8 polyhedra and $(Ta,Ti,Zr)O_6$ octahedra obtained in this study are shown in Fig. 5. The covalencies of Ta–O, Ti–O and Zr–O bonds in the $(Ta,Ti,Zr)O_6$ octahedra decreased with Zr substitution for Ti. The decrease in these cation-oxygen bonds is due to the increase in cation-oxygen bond length; the increase in the volume of $(Ta,Ti,Zr)O_6$ octahedra as mentioned above implies the increase in the cation-oxygen bond length. Although each of the covalencies of the cation-oxygen bonds in the $(Ta,Ti,Zr)O_6$ octahedra were decreased, the mean covalencies in the $(Ta,Ti,Zr)O_6$ octahedra were increased by the Zr substitution for Ti because

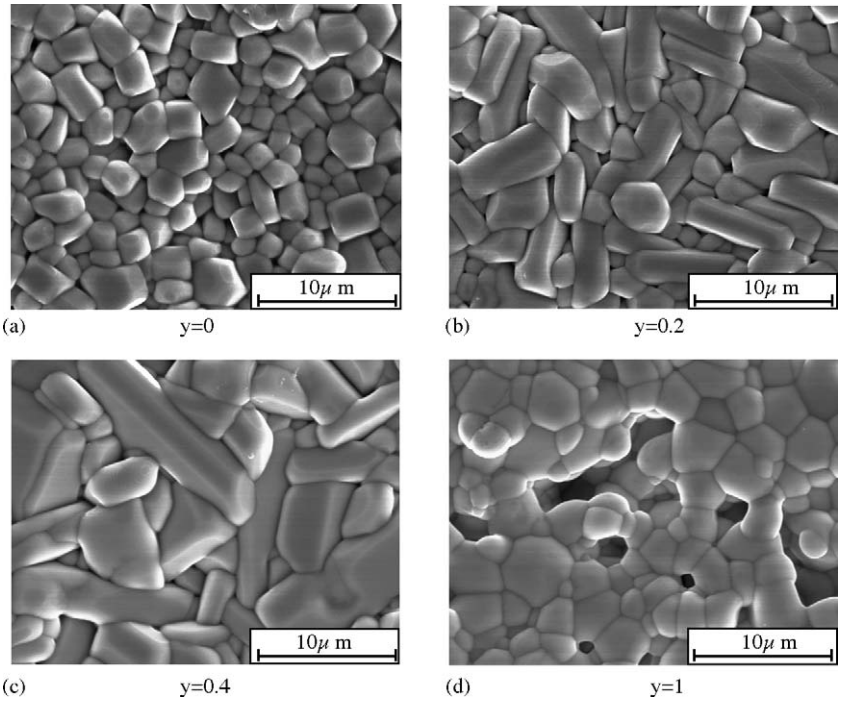

Fig. 8. FE-SEM photographs of $SmTa(Ti_{1-y}Zr_y)O_6$ ceramics at: (a) $y = 0$; (b) $y = 0.2$; (c) $y = 0.4$; and (d) $y = 1$.

the covalency of Zr–O bond is larger than that of Ti–O bond. As for the variations in the covalency of Sm–O bonds in the SmO_8 polyhedra, any significant variations in the covalency were not recognized; thus, this suggests that Zr substitution for Ti exerts an influence on the covalency of Ta–O, Ti–O and Zr–O bonds in the $(Ta,Ti,Zr)O_6$ octahedra.

The microwave dielectric properties of the $SmTa(Ti_{1-y}Zr_y)O_6$ ceramics are shown in Figs. 6 and 7. The dielectric constant of the samples in the single-phase region decreased from 37.6 to 28.9 with increasing composition y up to $y = 0.4$. This result is related to the increase in the mean covalency of cation-oxygen bonds in the $(Ta,Ti,Zr)O_6$ octahedra. The $Q \cdot f$ values of the samples increased from 24197 to 38320 GHz in the composition range of 0–0.4, whereas the $Q \cdot f$ values decreased at the compositions higher than $y = 0.4$; the results are shown in Fig. 6. The highest $Q \cdot f$ value, i.e., $Q \cdot f = 38320$ GHz, was obtained at $y = 0.4$. The microstructures of the samples were observed by using FE-SEM in order to evaluate the effect of Zr substitution for Ti on the microstructure. The FE-SEM photographs of the samples are shown in Fig. 8. The low $Q \cdot f$ value sample with the composition of $y = 0$ has very small grain size distributed in a range of 1–3 μm. Grain growth in the microstructure of the samples was observed with increasing composition y from 0 to 0.4; the increase in the $Q \cdot f$ values of the samples as mentioned above is related to the grain growth in the microstructure of the samples. However, as shown in Fig. 8(d), the grain size of the samples was decreased and porosity formation was observed at the composition $y = 1$. Thus, the decrease in the $Q \cdot f$ values of the samples at the higher composition than $y = 0.4$ is due to the decrease in the grain size and formation of porosity caused by formation of the secondary phases; the samples at the higher composition than $y = 0.4$ contained the $SmTaO_4$ and ZrO_2 phase as mention above. Moreover, the τ_f values of the samples ranged from 24.2 to −58.8 ppm/°C; a near zero temperature coefficient of resonant frequency was achieved at approximately $y = 0.3$ with the dielectric constant of 31.1 and $Q \cdot f$ value of 37481 GHz. Thus, it was found that a temperature-stable ceramic could be obtained by the Zr substitution for Ti.

4. Conclusion

The $Sm(Nb_{1-x}Ta_x)(Ti_{1-y}Zr_y)O_6$ ceramics were synthesized by the solid state reaction method and the relationships between the crystal structure and microwave dielectric properties were investigated. The $Sm(Nb_{1-x}Ta_x)TiO_6$ ceramics were single phase over the whole composition range, whereas the limit of solid solutions for $SmTa(Ti_{1-y}Zr_y)TiO_6$ ceramics was $y = 0.4$. The calculation of covalency of the cation-oxygen bonds showed a decrease in covalency of Ta–O, Ti–O and Zr–O bonds in the $(Ta,Ti,Zr)O_6$ octahedra and no significant variations in the covalency of Sm–O bonds in the SmO_8 polyhedra were observed. This suggests that Zr substitution for Ti exerts an influence on the covalency of cation-oxygen bonds in the $(Ta,Ti,Zr)O_6$ octahedra. Thus, a decrease in the dielectric constants of the $SmTa(Ti_{1-y}Zr_y)O_6$ ceramics with the Zr substitution for Ti could be related to the increase in the mean covalency of cation-oxygen bonds in the $(Ta,Ti,Zr)O_6$ octahedra. The $Q \cdot f$ values and τ_f values of the $SmTa(Ti_{1-y}Zr_y)O_6$ ceramics were improved by the Zr substitution for Ti. From the results, the optimum microwave dielectric properties were obtained for the $SmTa(Ti_{1-y}Zr_y)O_6$ ceramics; the properties at $y = 0.3$ are: $\varepsilon_r = 31.1$; $Q \cdot f = 37481$ GHz and $\tau_f = -2.2$ ppm/°C.

References

1. Vineis, C., Davies, P. K., Negas, T. and Bell, S., Microwave dielectric properties of hexagonal perovskites. *Mat. Res. Bull.*, 1996, **31**, 431–437.
2. Sebastian, M. T., Solomon, S., Ratheesh, R., George, J. and Mohanan, P., Preparation, characterization and microwave properties of $RETiNbO_6$ (RE = Ce, Pr, Nd, Sm, Eu, Gd, Tb, Dy, Y and Yb) dielectric ceramics. *J. Am. Ceram. Soc.*, 2001, **84**, 1487–1489.
3. O'Bryan Jr., H. M. and Thomson Jr., J., Phase equilibriums in the titanium oxide-rich region of the system barium oxide–titanium oxide. *J. Am. Ceram. Soc.*, 1974, **57**, 522–526.
4. Chang, P.-S., Dimorphs and isomorphs in $CeNbTiO_6$–$YNbTiO_6$. *Sci. Sin.*, 1963, **12**, 2337–2343.
5. Rietveld, H. M., Profile refinement method for nuclear and metal urinates. *J. Appl. Crystallogr.*, 1969, **2**, 65–71.
6. Izumi, F., In *Rietveld Method*, ed. R. A. Young. Oxford University Press, Oxford, 1993, Chapter 13.
7. Hakki, B. W. and Coleman, P. D., A dielectric resonator method of measuring inductive capacities in the millimeter range. *IRE Trans. Microwave Theory Tech.*, 1960, **MTT-8**, 402–410.
8. Shannon, R. D., Revised effective ionic radii and systematic studies of interatomic distance in halides and chalcogemides. *Acta Cryst.*, 1976, **A32**, 751–767.
9. Brown, I. D. and Shannon, R. D., Empirical bond-strength bond-length curves for oxides. *Acta Cryst.*, 1973, **A29**, 266–282.